Article published online: 2021-07-31

08-108

The Role Of Cardiac MRI In Congenital Heart Disease

MN SREE RAM, CM SREEDHAR, A ALAM, IK INDRAJIT

Abstract

Cardiac MRI is a valuable and an accurate modality used in the evaluation of structure and function of the heart. It is increasingly considered as a useful non invasive examination in management of cardiovascular conditions, a situation resulting from significant advances in MR technologies. Evaluation of congenital heart disease is an important application of Cardiac MRI since the morphological details of chambers, septum, defects and anomalous connections are depicted accurately. Additionally, flow information across valves, chambers, outflow tracts and shunts are also provided. Its utility is further increased especially during follow up of patients after corrective surgery. This article reviews current state-of-the-art MRI application in common congenital heart diseases.

Ind J Radiol Imag 2005 15:1:239-246

Key words : - Cardiac MRI; Congenital Heart Disease; Septal defects

INTRODUCTION

Congenital heart disease is a common clinical entity and occurs in 0.8 % of live newborns [1]. While many newborns and children undergo surgical procedures, nearly 50,000 adults with congenital heart disease have surgically treated and at least 150,000 adults fall into a large subset of unrecognized, misdiagnosed and undiagnosed but untreated category. [2] [3] [4]. In recent times, Cardiac MRI has emerged as an accurate method for the evaluation of structure and function of the heart. Its widespread use in clinical practice has been due to significant advances in MR technology like the emergence of high-field-strength magnets, high-performance gradient hardware, and ultrafast pulse sequences [5]. When these advances augment traditional techniques like cardiac gating, suspension of breathing, adaptation to diaphragmatic motion, the final outcome is better anatomical and functional images of the heart obtained in faster times.

Cardiac MR imaging is never considered as an initial imaging strategy in congenital heart disease, but advantages like generation of high-resolution images in any orientation, creation of cine images of the heart and angiographic images of aorta, pulmonary arteries, systemic and pulmonary veins, makes it a valuable tool [6]. The MRI protocol for pediatric congenital heart disease comprises of anatomic and physiologic components. ECG-gated spin-echo imaging and Contrast enhanced MR angiography is used for anatomic information, while functional information is obtained from Cine Trufi (steady-state free precession), Cine Flash (gradient-echo) and Cine phase-contrast sequences. These protocols provide complementary data of the morphology of cardiac and extra cardiac anatomy as well as the functional information across ventricles, valves, shunts, defects and connections [7]. While spin echo techniques focuses on morphology due to its high contrast resolution, gradient echo techniques focus on functional information by acquiring series of images during cardiac cycle that reflects its high temporal resolution [7].

MATERIAL AND METHODS

Patient Population

Twenty six patients with an age range 1½ to 38 years with congenital heart disease underwent MR imaging at our Institute from Jan 2003 to Jul 2004. There were 10 male and 16 female patients. Four patients of Tetralogy of Fallot were scanned before and after surgery. In all patients, the abnormalities were demonstrated previously by echocardiography except the cases of coarctation of aorta while 11 patients had an angiography prior to MRI. The true diagnosis was considered to be the findings shown by 2D echocardiography excepting coarctation cases. MR imaging was performed using a 1.5 T (Magnetom Symphony with Quantum gradients [maximum gradient amplitude, 30 mT/m; slew rate, 125 mT/m/sec]; Siemens Medical Systems, Erlangen, Germany) with use of an integrated body coil.

Patient preparation

A detailed history was elicited from each patient including principal symptoms and signs, echocardiographic and

From the Dept of Radiodiagnosis, AMFC, Pune

Request for Reprints: Col M. N. Sreeram, Prof & Head, Dept of Radiodiagnosis, AFMC, Pune - 411 040

Received 6 August 2004; Accepted 10 February 2005

cardiac catheterization data, and operative status. The patient particulars and the details of congenital heart disease analyzed in this study are displayed in Table 1. For all patients in this study, MR-compatible electrocardiographic leads were placed on the anterior chest wall before imaging and attached to the MR imaging unit for electrocardiographic gating. ECG leads were positioned on posterior chest wall when less motion artifact was needed. For most sequences, electrocardiographic triggering was used to synchronize imaging with the onset of systole and offset cardiac motion and match each image to the desired cardiac phase. The referring physician and anesthetist were consulted for the type of sedation (general anesthetic sedation, deep sedation, or conscious sedation) for every case. The sedation techniques included medication by midozalem, ketamine injection or propafol infusion. The exam commenced with an integrated body array coil. Scans were performed generally using non breath holding techniques, with few cases undergoing breath-holding scan techniques based on precise monitoring of diaphragmatic motion.

Cardiac MRI Protocol

In our institute, the MR imaging protocol commenced with a localizer using Trufi (steady-state free precession) sequence. A list of protocol is given as Table 2. Axial and Coronal scans of 10 mm thickness using HASTE were obtained with acquisition extending from the level of aortic arch to below the diaphragm including the inferior venal cava and hepatic veins. It was useful in demonstrating ventricular and atrial septal defects as well as providing anatomical landmark for deriving oblique sections, subsequently. From the localizer, vertical long axis, short axis and horizontal long axis were obtained. The anterior slices during planning of horizontal long axis generated a left ventricular outflow tract image. Functional analysis was performed using a combination of Cine Trufi (steady-state free precession), Cine Flash (gradient-echo) and Cine phase-contrast sequences. In few cases a three point technique determined the right ventricular outflow tract. For evaluation of aorta, pulmonary trunk, coronal view was useful.

Results

The study comprised of 30 Cardiac MRI studies performed on 26 patients with congenital heart disease. The age range was 1½ to 38 years. There were 10 male and 16 female patients (Table 1). 13 studies were performed in 9 patients with tetralogy of Fallot, including four studies done on cases before and after surgery. In this study, tetralogy of Fallot was the commonest congenital heart disease evaluated by MRI. Among the patients who underwent surgery, three were treated by palliative repair and one by corrective repair. The other cases in this study, consisted of 6 cases of ASD, 3 cases of VSD, PDA and Coarctation each, 1 case of Truncus Arteriosus and Single ventricle.

Data Collection and Image Analysis

MR Images were reviewed retrospectively by a panel of four radiologists. The images of each patient were analysed to define cardiovascular anomalies. The morphological information comprised of chamber and valve anatomy, structure and integrity of septum, alignment and caliber of outflow tracts and atrioventricular connections The functional information comprised of quantification of flow across valves, outflow tract and defects. Quantification of systemic and pulmonary flow was done in cases of septal defects. Cine imaging in horizontal long-axis provided dynamic information of the cardiac size, valve morphology, leaflet mobility, wall thickness, chamber size, flow jets and outflow tracts. Cine imaging in vertical long-axis offered information on chambers size, septum anatomy, defect morphology and aortopulmonary connections.

DISCUSSION

Cardiac MR imaging is considered as a valuable modality for evaluation of congenital heart disease [7] [8]. Cardiac MR imaging has much to offer by a) generating high resolution morphological images, b) offering quantitative information of the severity of regurgitant or stenotic lesions with peak velocity and flow measurements and c) quantification of shunt. The greatest challenge of cardiac MR imaging is motion artifact from the heart, adjacent vascular structures, and respiration [9]. With the ongoing developments in gradient hardware and pulse sequence technology, imaging sequences that can "freeze" the motion of the heart during the cardiac cycle is now available [5]. Moreover, with the development of rapid pulse sequences, breath-hold imaging is facilitated, which is necessary to accommodate the wide range of motion the heart undergoes during respiration.

The indications for MRI in the evaluation of patients with congenital heart disease have been now determined [10]. The major indications at the moment includes: 1) segmental description of cardiac anomalies; 2) evaluation of thoracic aortic anomalies; 3) noninvasive detection and quantification of shunts, stenoses, and regurgitations; 4) evaluation of cono-truncal malformations and complex anomalies; 5) identification of pulmonary and systemic venous anomalies; and 6) postoperative studies.

Atrial septal defects (ASD) occur in 10% of congenital heart disease and are the most common type of CHD to present in adult life. Three main types of ASD are commonly seen: secundum (in middle of atrial septum), which is the commonest, sinus venosus (at junction of SVC and right atrium superiorly), and primum (in inferior

Table 1: Cardiac MRI for Congenital Heart Disease : Patient details (n=30)

Clinical Diagnosis	No cases	No	Name	Age	Sex	Clinical Px	Operative Status at time of MRI Study	MRI Diagnosis	Special Findings
TOF	8	1	so SDT	5	M	Cyanosis	None	TOF	
		2	d/o SR	5	F	Cyanosis	None	TOF	MAPCA
		3	s/o PFK	1½	M	Failure to thrive	None	TOF	
		4	d/o SL	5	F	Cyanosis	None	TOF	
		5	d/o MNN	4	F	Cardiac Murmur	None	TOF	Scoliosis
		6	d/o GL	3	F	Cyanosis	None	TOF	
		7	d/o JNS	6	F	Tiredness	None	TOF	
		8	d/o RNG	4	F	Tiredness	None	TOF	
TOF Optd	5	1	s/o K	4	M	Follow Up	BT	TOF Optd	
		2	d/o JNS	6	F	Symptom Recurrence	BT Shunt Blockage	Shunt Blockage	Left sided SVC
		3	s/o SDT	5	M	Follow Up	BT	TOF Optd	
		4	d/o GL	3	F	Follow Up	Corrective Surgery	TOF Optd	
		5	d/o RNG	4	F	Shunt Blockage	BT Shunt Blockage	TOF Optd	Shunt Blockage
ASD	6	1	I	16	F	Breathlessness	None	ASD	
		2	w/o RK	34	F	Asymptomatic	None	ASD	
		3	S N	27	M	Pulmonary Hypertension	None	ASD	
		4	d/o N	7	F	Mitral Valve Prolapse	None	ASD	
		5	d/o PL	8	F	Cyanosis	None	ASD	
		6	w/o BS	28	F	Breathlessness	None	ASD	
VSD	3	1	D/o LNM	3	F	Failure to thrive	Repair	VSD Optd	
		2	s/o DPN	8	M	Cardiac Murmur	None	VSD	
		3	S P	10	M	Tiredness	None	VSD	
PDA	3	1	PS	8	M	Cardiac Murmur	None	PDA	
		2	s/o SK	5	M	Failure to thrive	None	PDA	
		3	d/o AJ	4	F	Cardiac Murmur	None	PDA	
Coarctation	3	1	w/o PS	38	F	Hypertension	None	Coarctation	Capture of Left SCA
		2	w/o M	26	F	Weakness	None	Coarctation	
		3	VK	29	M	Radiofemoral delay	None	Coarctation	
Truncus Arteriosus	1	1	s/o N	8	M	Cyanosis	None	Truncus	Truncus Type 1
Single Ventricle	1	1	P	15	F	Cyanosis	None	Single Ventricle	Left Ventricular
Total	=	30							

n

Table 2. Generic Protocol for Common Sequences in Cardiac MRI

Description	Morphology	Morphology	Dynamic	Dynamic	Dynamic	Contrast MRA
Pulse Sequence	TSE	FLASH	Cine FLASH Breath Hold	Cine FLASH NonBreath Hold	Cine True FISP	Gradient Echo
Plane	Tra , Cor	Short Axis Long Axis	Short Axis Long Axis LVOT / RVOT	Short Axis Long Axis LVOT / RVOT	Short Axis Long Axis LVOT / RVOT	Long Axis Coronal
Flip angle	160^0	30^0	30^0	25^0	65^0	^{0}
TR (msec)	800	84	69	40	55	140
TE (msec)	26	4.2	4.2	4.2	1.8	6
NSA	1	1	1	3	1	1
Concatenations	2	1	1	1	1	1
FOV Read (cm)	340	320	380	340	340	300
FOV Phase (cm)	70	80	82	82	75	82
Number of Slices	14	1	1	4	1	1
Slice thickness (mm)	8	7	6	6	6	5
Matrix	256 x 56	256 x 94	256 x 60	256 x 60	256 x 62	256 x 68
Acquisition Time						
No of sections	14	1	1	4	1	1
No of seconds	11 s	16 s	16 s	5 min	6 s	13 s
Other Parameters	Turbo Factor 99 99					0.1-0.2 mmol/kg Timing by test dose

TI = inversion time, TE = echo time, TR = repetition time, NSA = number of signal averages; TSE = Turbo Spin Echo, FLASH = Fast Low Angle Shot , True FISP = True fast imaging with steady-state precession IR = inversion recovery

FOV was modified in individual cases based on body size

portion of atrial septum, near atrioventricular valves). MRI shows a defect on two adjacent axial images or during multiple phases of the cardiac cycle during cine imaging at one anatomic level [11] and effects of left-to-right shunting in form of right atrial and ventricular volume overload. The sensitivity and specificity of MRI for the diagnosis of ASD are both > 90% [12]. The defect is best seen in horizontal long axial and oblique sagittal sections, as was evident in this study [Figure 1]. To overcome the limitation of normal thinning at region of secundum, the defect should be identified in two or more sections reinforced by correlation with right sided volume loading. The dilated right chambers rotate the heart into the left chest across the midline with interventricular septum nearly in the coronal plane. An important finding in ASD presenting in adults is pulmonary hypertension which occurs in 40 % cases, mostly due to increased flow. Mitral valve prolapse and mitral regurgitation occurs occasionally.

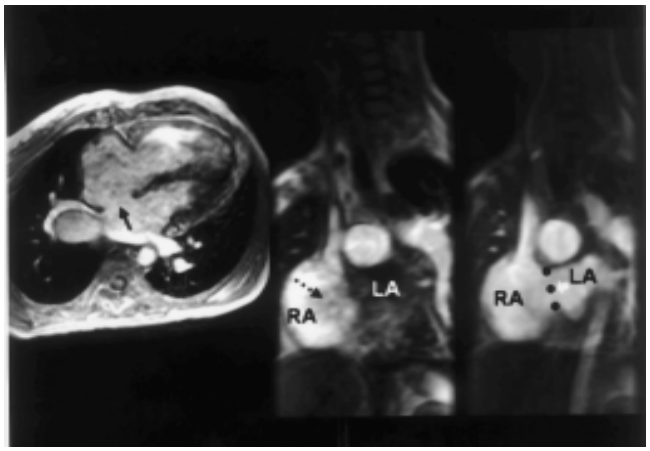

Figure 1: Atrial Septal Defect : Clockwise from left : Cine Flash MR in four chamber view of a 34 year old lady with a large atrial septal defect shows a discontinuity in the interatrial septum (black arrow). Note the dilated right atrium, right ventricle, and lower lobe pulmonary veins. The heart is rotated into the left chest. The left atrium is normal in size. "Freeze Frame" Contrast enhanced MRA in coronal plane reveals opacification of right atrium and pulmonary trunk, with unopacified blood from left atrium entering through the defect (black arrow). Image obtained 5 seconds later shows opacification of both atrium, with shunting of blood from left to right. Note the true size of the defect in coronal plane represented by dotted lines.

Ventricular Septal Defect (VSD) is a common congenital heart disease which is typically classified into membranous (70-80%), muscular (10%), endocrinal cushion defects (5-10%) and conal (5%). MRI findings include a defect in the above locations, increased vascularity with a 2:1 or greater shunt, cardiomegaly and enlarged left atrium. While 30-40% of patients close spontaneously, infants can present with congenital heart failure at 2-3 months. Surgical approaches advocated are closure in membranous type and ventriculotomy in muscular type. The defect is best seen in axial and coronal images. Small defects which are difficult to detect, can be better delineated by angulated sections and reconstructions. Cine gradient echo images can differentiate left to right, right to left and bidirectional shunts. In this study, there were 3 patients with a VSD. The defect was identified correctly in all 3 on horizontal and vertical long axis views. There was straightening of the ventricular septum in 1 case. The dilatation and hypertrophy of right ventricle was identified on axial images in all cases.

Tetralogy of Fallot (TOF) is the commonest cyanotic congenital heart disease. Described first by Stensen, a Danish anatomist in 1671, and subsequently by Fallot, a French physician in 1888, it is a combination of overriding of aorta, VSD, infundibular pulmonary stenosis, and right ventricular hypertrophy. MRI demonstrates all findings in this condition includes infundibular stenosis, ventricular septal defect [Figure 2] which is either membranous or / muscular beneath crista, pulmonary valve anomalies like bi/unicommissural valves, large right pulmonary artery and right aortic arch. Among the right aortic arch, 90% present with mirror imaging branching of the great vessels, while the remaining 10% have an aberrant left subclavian artery. Associated anomalies that can occur include MAPCA's (major aortopulmonary collateral arteries), peripheral pulmonary artery coarctation, coronary artery anomalies like anomalous LAD arising from right coronary artery.

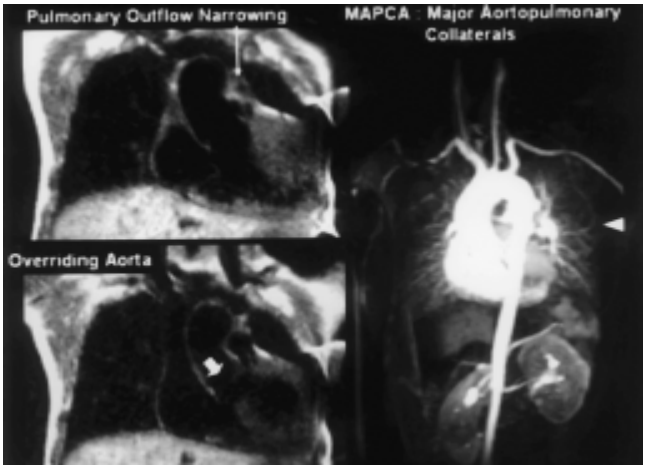

Figure 2: Tetralogy Of Fallot: Coronal T1 turbo SE MR Images in a 5 year old girl with tetralogy of Fallot shows presence of stenosis of infundibulum at left panel (white arrow) and overriding of the aorta (white block arrow) with maintained mitral-aortic continuity. Contrast enhanced MRA shows the presence of MAPCA's (major aortopulmonary collateral arteries) (white arrowhead), which are variable in number, size and location and are the main source of pulmonary blood supply.

MRI is also excellent for evaluating both palliative and corrective surgical repair that have effectively resulted in improved long term survival [13]. Palliative shunt corrections between the systemic and pulmonary circulations include Blalock-Taussig shunt (described first in 1944) between subclavian artery to pulmonary artery, Waterston shunt connecting descending aorta to left pulmonary artery and Potts shunt linking ascending aorta

to right pulmonary artery. However, due to the fixed size of shunt conduit, children often outgrow them 2 years after the procedure, and definitive repair is usually performed at 5-7 years which consists of pericardial patching the VSD and wide reconstruction of the RV outflow tract to relieve the pulmonary outflow obstruction. Corrective repair entails relieving the right ventricular outflow obstruction with reconstruction and patch closure of the ventricular septal defect in corrective surgery. During follow up period, MRI can provide useful information on adequacy of pulmonary circulation and the presence of pulmonary regurgitation [14]. Pulmonary regurgitation is a complication of surgical reconstruction of the outflow tract which does not have a valvular apparatus. Consequent to regurgitation, there is an increase in end-diastolic volume of the right ventricle, which on MRI is seen as right ventricular outflow dilatation and right ventricle hypertrophy [15].

Patent ductus arteriosus (PDA) is the persistence of the sixth aortic arch and accounts for about 10% of congenital heart disease. The ductus arteriosus is a fetal connection between origin of the left pulmonary artery to the descending aorta just beyond the origin of the left subclavian artery. It closes soon after birth due to a decrease in pulmonary arterial pressure and contraction of the muscles in the duct wall. A persistent communication is the hallmark of this condition.. When the ductus arteriosus remains patent, blood is shunted from the aorta to the left pulmonary artery [Figure 3] with enlarged left atrium and ventricle. MRI is useful in showing either the presence of an isolated PDA or as an association with other heart diseases like VSD, coarctation of the aorta, hypoplastic aortic arch, single ventricle and pulmonic stenosis.

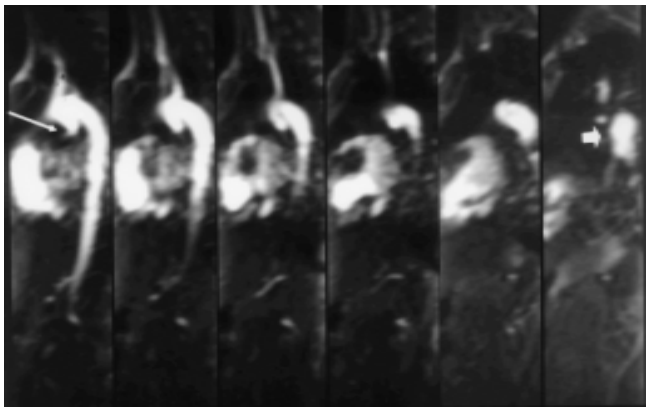

Figure 3: Patent Ductus Arteriosus: "Freeze Frame" Contrast enhanced MRA in a 8 year girl with patent ductus arteriosus. Reconstructed images in coronal plane reveals left sided PDA connecting undersurface of arch of aorta (white arrow) to the left pulmonary artery (block arrow). Note the wide origin of the left-sided PDA which termed as the ductus infundibulum.

Coarctation of the aorta (CoA) is a congenital narrowing of the aorta, occurring just distal to the left subclavian artery. The narrowing is proximal, adjacent, or distal to the site of entry of the ductus arteriosus, or insertion of the ligamentum arteriosum. There are two presentations: infantile and adult. The infantile type is associated with a VSD in 50% of cases and a patent ductus arteriosus in 30% which supplies blood to the descending aorta beyond the area of narrowing. The adult type presents with systemic hypertension, aortic dissection, stroke, heart failure and endocarditis. MRI is useful in diagnosis of coarctation, in presurgical planning, and during post surgical follow-up [16]. Preoperatively, MRI offers useful information on location, extent and severity of the narrowed aortic segment, besides mapping the collateral pathways. The coarctation segment is best seen on oblique coronal and sagittal images [Figure 4]. Changes in arch of aorta like hyperplasia of distal aortic arch and proximal descending aorta, shortened AP dimensions, cepahalad extension of arch and curved and 'captured' origin of left subclavian artery can be demonstrated. The collateral circuits of coarctation seen on MRI include dilation of both subclavian, internal mammary, intercostals, dorsal scapular and epigastric arteries. Cine PC imaging quantifies the pressure gradient across the coarctation.

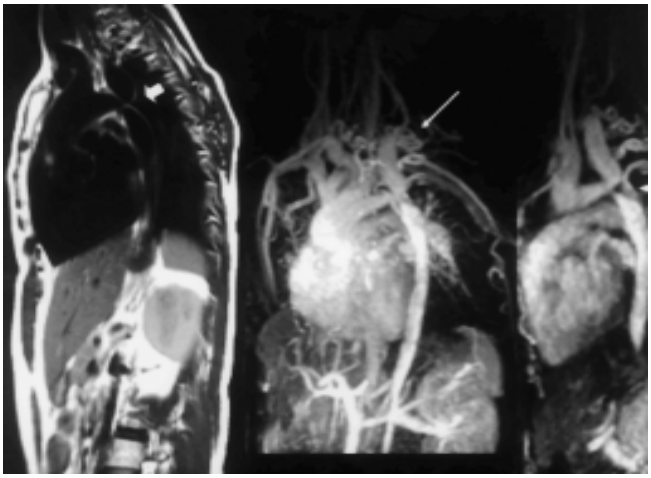

Figure 4: Coarctation of Aorta: Oblique Coronal TSE MRI Images in a 38 year hypertensive female shows significant narrowing of the aorta (white block arrow) distal to origin of left subclavian artery. Contrast enhanced MRA reveals delineation of the aortic arch and its branches. Numerous collaterals are present involving the intercostals (white arrows), internal mammary and dorsal scapular arteries, diverting blood flow to lower body and lower limb. Delayed phase reveals increased opacification of the thoracic aorta distal to the coarctation (white arrowhead), due to incoming blood from the intercostals.

Single ventricle (SV) belongs to a category of cyanotic malformations, termed admixture lesions, because of mixing of venous and arterial blood within the heart and great arteries. In this condition, both atria and their AV valves communicate with a single ventricle [Figure 5] [17]. It is also synonymously called as primitive ventricle, common ventricle, double or single inlet left or right ventricle, cor biloculare and triloculare. There are three

cardinal morphologic characteristics of single ventricle : a). most commonly, of a left ventricle type, b) right ventricle type and c) rarely a common ventricle type with a rudimentary septum in the ventricular cavity. The Fontan surgical procedure and its modifications are designed to direct total systemic venous return to the lungs. It is used for the treatment of single ventricle, and a number of other complex cardiac malformations like tricuspid atresia,. [18]. Currently, the most frequently used type of Fontan operation involves the installment of a total cavopulmonary connection, excluding the right ventricle.

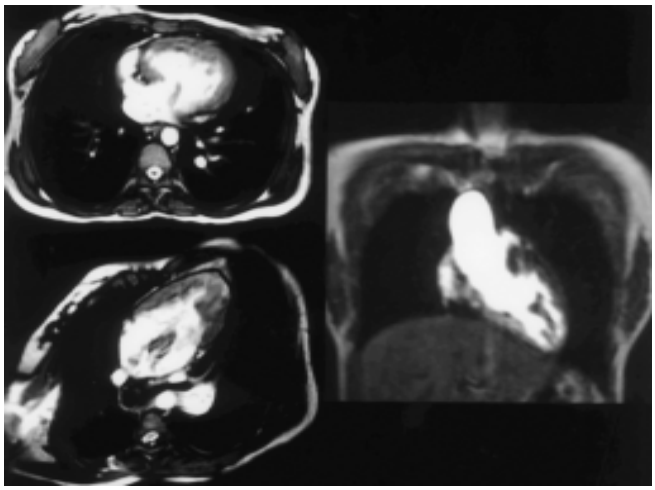

Figure 5: Single Ventricle: Cine Trufi in axial and horizontal long axis plane in a 15 year old cyanotic girl shows evidence of a single ventricle, characterized by a "right ventricle" morphological pattern. Contrast enhanced MRA shows at right panel reveals the connection between the single ventricle and the ascending aorta and aortic arch

Truncus Arteriosus (TA) is an uncommon condition, occurs in 2% of CHD, presenting with common aorticopulmonary trunk, due to a failure of splitting of the primitive common truncus arteriosus into aorta and pulmonary artery by a spiral septum. It is associated with a large, high riding VSD [Figure 6A] and an ASD can occur in about 20% of cases. The common truncal valve typically has 3 cusps in 70% of cases, but can vary from 2 to 6, with possible stenosis or insufficiency at this valve. Associated cardiac abnormalities include a right aortic arch, coronary artery origin anomalies and persistent left SVC. Rastelli procedure is the treatment of choice, with reconstruction of pulmonary outflow tract via a RV to pulmonary artery synthetic graft. Truncus Arteriosus is classified into 4 types:Type 1 (pseudopulmonary trunk) is the commonest, accounting for 70% of cases and denotes a common truncal vessel giving off a well formed main pulmonary artery which bifurcates into right and left pulmonary arteries. Type 2 has separate left and right pulmonary arteries arising directly from dorsal surface of the ascending truncal vessel. Type 3 has separate left and right pulmonary arteries arising from lateral surface of the ascending portion of the truncal vessel. Type 4 is essentially called pseudotruncus occurring due to pulmonary conal agenesis, rather than failure of truncal septation. There is no right ventricle to pulmonary artery communication. In this study, there was one case of Truncus Arteriosus, exhibiting Type 1 / pseudopulmonary trunk features [Figure 6B].

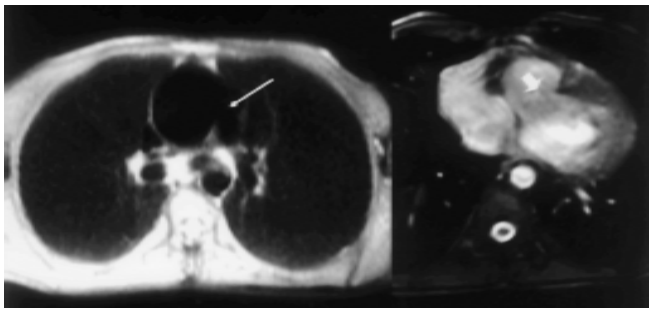

Figure 6A: Truncus Arteriosus: Axial T1 MRI sequences in a 8 year cyanotic boy shows a single arterial vessel at the base of the heart without a distinct and separate aorta or pulmonary trunk from which the aortic arch, pulmonary, coronary arteries originate. White arrow points to the origin of pulmonary arteries from the left inferior base of this common trunk, classifying it as a Type I of Truncus Arteriosus. Oblique Cine Flash MRI images shows a large VSD (white block arrow)

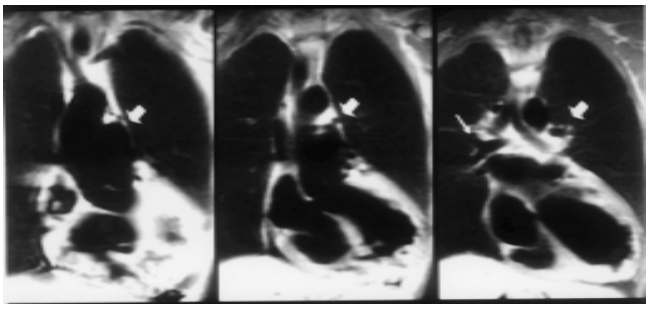

Figure 6B: Truncus Arteriosus:
Panel of Coronal T1 MRI sequences in same patient shows the pulmonary arteries (white block arrows) to originate from the left inferior aspect of the common arterial trunk with a short main stem, classifying it into type I Truncus Arteriosus.

Few areas of difficulties are present inherently in Cardiac MRI, which can be overcome by a series of measures [9]. Firstly, a vast number of imaging techniques are available and by experience the radiologist must choose the optimal set of MRI protocols to evaluate specific pediatric cardiac problems. Secondly, cardiac arrhythmias can interfere in MR acquisition resulting in sub optimal and non conclusive studies. Thirdly, breath hold sequences may be difficult to perform in a setting of infants with cyanosis and respiratory distress, adversely affecting the use of Trufi and other cine sequences. Fourthly, distal pulmonary artery branch stenosis may not be delineated, a critical information during follow up of cases with Tetralogy of Fallot. Notwithstanding the above, Cardiac MRI has however emerged as an accurate method for the evaluation of structure and function of the heart.

Conclusion

Cardiac MRI has emerged as a useful technique in evaluation of congenital heart disease. It is being increasingly considered useful as a "one-stop" comprehensive examination [5] in the diagnosis of morphologic and functional evaluation in presurgical planning, and during post surgical follow-up of congenital heart diseases. In practice, Cardiac MRI protocol for congenital heart disease typically comprises of anatomic and physiologic components. It is expected that continuing advancements in gradient and fast scanning technologies will further push the frontiers of Cardiac MRI applications, especially in follow up of patients undergoing surgical repair.

REFERENCES

1. Mitchell SC, Korones SB, Berendes HW: Congenital heart disease in 56,109 births. Circulation 1971;43:323-332 .
2. Joyce L: Mended hearts grow up. Stanford Med 1994;11:18-25.
3. Perloff JK: Overlooked congenital heart disease in the adults: Part 1. J Cardiovascular Med 1980;5:535-545
4. Perloff JK : Overlooked congenital heart disease in the adults: Part II. J Cardiovascular Med 1980;5:550-562
5. Reeder SB, Du YP, Lima JAC, Bluemke DA: Advanced Cardiac MR Imaging of Ischemic Heart Disease. Radiographics 2001; 21:1047-1074
6. Glockner JF, Johnston DL, McGee KP: Evaluation of cardiac valvular disease with MR imaging: qualitative and quantitative techniques. Radiographics. 2003;23(3):686-693
7. Wimpfheimer O, Boxt LM: MR Imaging of Adult patients with Congenital Heart Disease. Radiol Clin North Am 1998; 37:421-437.
8. Didier D, Higgins CB, Fisher MR, et al: Gated magnetic resonance imaging in congenital heart disease: experience in initial 72 patients. Radiology 1986; 158:227-235.
9. Boxt LM. Cardiac MR Imaging: A guide for beginners. Radiographics 1999;19:1009-1025
10. Task Force of the European Society of Cardiology, in collaboration with the Association of European Pediatric Cardiologist: The clinical role of magnetic resonance in cardiovascular disease. Eur Heart J. 1998;19:19-39.
11. Wexler L, Higgins CB, Herfkens RJ : Magnetic resonance imaging in adult congenital heart disease. J Thorac Imaging. 1994;9:219-229.
12. Diethelm L, Dery R, Lipton MJ, et al.: Atrial level shunts: Sensitivity and specificity of MR diagnosis. Radiology. 1987;162:181-186.
13. Panigrahy A, Ratib O, Boechat MI, Gomes AS: Advances in magnetic resonance imaging of pediatric congenital heart disease. Applied Radiology 2002; 107(S):103-111.
14. Helbing WA, de Roos A: Clinical applications of cardiac magnetic resonance imaging after repair of tetralogy of Fallot. Pediatr Cardiol. 2000; 21:70-79.
15. Rebergen SA, Chin JGJ, Ottenkamp J, van der Wall EE, de Roos A: Pulmonary regurgitation in the late postoperative follow-up of tetralogy of Fallot: volumetric quantitation by nuclear magnetic resonance velocity mapping. Circulation 1993; 88:2257-2266.
16. Fawzy ME, von Sinner W, Rafai A, et al. MRI compared with angiography in the evaluation of intermediate-term results of coarctation balloon angioplasty. Am Heart J. 1994;126:1380-1384.
17. Marin-Carcia J, Tandon R, Moller JH et al: Single ventricle with transposition. Circulation 1974; 49:994 -8.
18. DeLeon SY, Ilbawi MN, Idriss FS et al: Fontan type operation for complex lesions. J Thorac Cardiovasc Surg 1986; 92:1029-1037